

Nanoporous Carbon Nanotubes Synthesized through Confined Hydrogen-Bonding Self-Assembly

Adrian T. Rodriguez,[†] Min Chen,^{†,‡} Zhu Chen,[†] C. Jeffrey Brinker,^{†,‡} and Hongyou Fan^{*,†,‡}

Department of Chemical and Nuclear Engineering and UNM/NSF Center for Micro-Engineered Materials,
The University of New Mexico, Albuquerque, New Mexico 87131, and Chemical Synthesis and Nanomaterials
Department, Advanced Materials Laboratory, Sandia National Laboratories, 1001 University Boulevard,
Albuquerque, New Mexico 87106

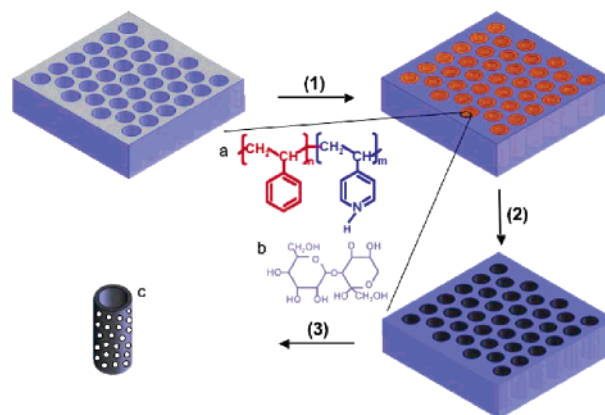
Received February 27, 2006; E-mail: hfan@sandia.gov

Carbon nanotubes have received great attention due to their unique optical, electrical, and mechanical properties and their potential applications in nanoelectronics, sorption, and gas sensing since their invention in 1991.^{1–4} Several direct methods have been developed for the synthesis of carbon nanotubes, including dc arc-discharge, laser ablation, and chemical vapor deposition.² Recently, templating methods have been developed to synthesize carbon nanotubes by carbonization of either polymer or pre-organized disclike molecules in porous anodic aluminum oxide (AAO) membranes.⁵ In general, the carbon nanotubes synthesized using the above methods exhibit either graphite-structured or amorphous tube walls with microporosity (pore size in the wall <0.5 nm). In many applications, such as macromolecule sorption, separation, and sensing, carbon nanotubes with larger pores in the tube wall are preferred. Hyeon et al.⁶ synthesized hollow carbon tubes with randomly distributed 4-nm pores in the tube wall and rectangular-shaped channels using mesoporous silica tubes as templates. However, this method has several limitations. First, it is not easy to synthesize tubular silica templates. It is even more difficult to control the tube diameter, length, and pore size in the wall. Second, the infiltration of carbon precursors into the templates relies on capillary forces that cannot guarantee complete filling of the mesopore and the entire silica tube wall. Thus, after removal of silica templates, some of the resulting carbon tubes have unconnected pores and irregular shapes. Third, pore size control in the mesoporous carbon tube wall is very limited (<5 nm).

Here we report a simple and direct synthetic method for the preparation of nanoporous carbon nanotubes with larger pores (>10 nm) on the tube wall. The method combines the use of AAO as a template for the tube diameter and block copolymer/carbohydrates self-assembly within thin films confined inside AAO pore channels to form nanopores. It involves coating the AAO inner pore channel surface with block copolymer (polystyrene-*co*-poly(4-vinylpyridine), PS-PVP) and carbohydrates in dimethylformamide (DMF) solution (see Scheme 1, see Supporting Information for detailed synthesis). Drying of DMF induced microphase separation of PS-PVP and formation of ordered PS domains and PVP/carbohydrate domains. After carbonization at high temperature (>460 °C) in argon, PS was removed, forming the mesopores; carbohydrates and PVP were carbonized, forming the framework of nanoporous carbon tubes within AAO channels. Removal of AAO led to the formation of individual monodisperse nanoporous carbon nanotubes.

Figure 1 shows representative SEM images of the resulting mesoporous carbon nanotubes. The nanotubes are straight and monodisperse with ~200 nm diameter. The high-resolution SEM (Figure 1b) shows that they have open ends. TEM images (Figure

Scheme 1. Schematic Illustrations of the Synthesis of Nanoporous Carbon Nanotubes through AAO Confined Hydrogen-Bonding Self-Assembly^a



^a Conditions: (1) infiltration of the polymer and carbohydrate DMF solution into the AAO templates; (2) carbonization in argon; (3) removal of AAO templates and formation of individual nanoporous carbon nanotubes (c); (a) poly(styrene)-*co*-poly(4-vinylpyridine) (PS-PVP); (b) carbohydrates such as turanose, raffinose, glucose, etc.

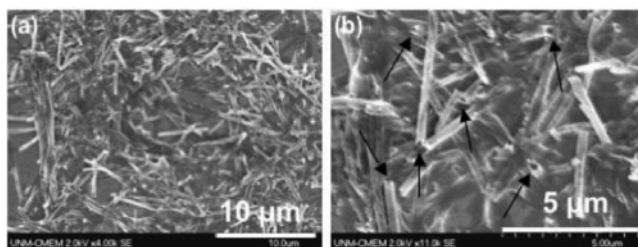


Figure 1. Scanning electron microscopy (SEM) images of nanoporous carbon nanotubes carbonized at 600 °C in argon. The sample was prepared using PS-P4VP. (a) Low-resolution SEM image. (b) Magnified SEM image of the sample in (a). Arrows point to the open ends of nanotubes.

2a and inset) revealed that the nanotube wall was nanoporous in the tube wall. The tube wall is about 15 nm thick. No graphitic microstructure was observed in the HRTEM, which suggests that the pore wall is amorphous carbon. ¹³C NMR spectra show a single resonance at $\delta = 110.6$ ppm, suggesting the existence of sp²-type carbon species. N₂ isotherms on these nanotubes showed a surface area of 130 m²/g with large mesopores with an average size of ~16 nm (Supporting Information). In addition to straight tubes, branched tubes were also observed (Figure 2b), probably due to the intrinsic defects on the AAO membrane. This suggests that the PS-P4VP/carbohydrate coating completely covered the AAO pore channel surface.

Figure 2c shows the TEM images of bamboo-like tubes. These tubes were produced when the PS-P4VP/carbohydrate-coated AAO

[†] The University of New Mexico.[‡] Sandia National Laboratories.

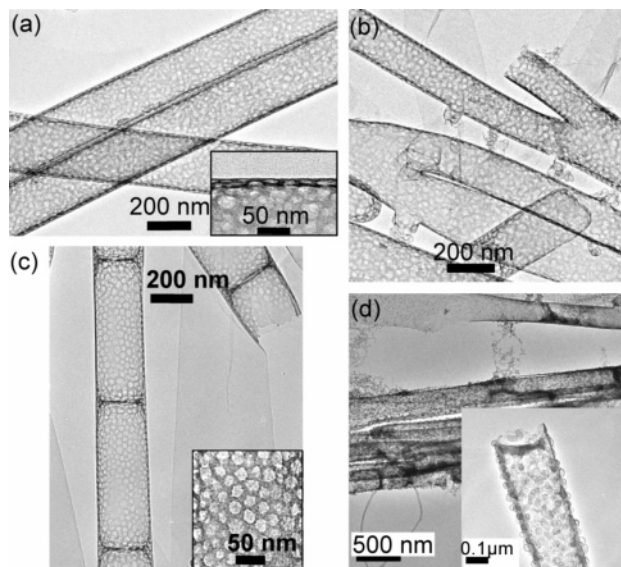


Figure 2. Transmission electron microscopy (TEM) images of nanoporous carbon nanotubes. (a) The same sample as in Figure 1a. Inset: Magnified image over a nanotube wall, showing the nanoporous feature within the tube wall. (b) TEM image of branched nanotubes. (c) TEM images of bamboo-like nanotubes. Inset: Hexagonal arrays of pores on the tube wall. (d) TEM images of carbon nanotubes prepared using PS-P2VP. Inset: High-resolution TEM image of same sample.

membranes were annealed at 80 °C in benzene/DMF vapor overnight. In this case, the nanopores are distributed much more uniformly on the tube surface than those of un-annealed samples, forming ordered hexagonal arrays. By using block copolymer with different PVP blocks (e.g., P2VP), we were able to tune pore structures in the tube wall and tube surface architectures. As shown in Figure 2d, carbon nanotubes prepared using PS-P2VP have a rough tube surface, in contrast with the smooth and nanoporous tube surface prepared using PS-P4VP. Individual hollow carbon particles are uniformly distributed on the tube surface.

Similar to the confinement of block copolymer self-assembly,^{7–10} the formation of nanoporous carbon nanotubes is a confined hydrogen-bonding self-assembly process. The hydrogen bonding between carbohydrates (hydroxyl groups) and pyridine blocks (nitrogen groups) has been confirmed by FTIR characterizations of pure PS-P4VP and PS-P4VP/carbohydrate coating (Supporting Information). In comparison with the spectra of pure PS-P4VP, the P4VP characteristic peaks from PS-P4VP/carbohydrate coating at 1597, 1415, and 993 cm^{-1} have shifted, suggesting the formation of hydrogen bonding between the hydroxyl groups from carbohydrates and nitrogen groups from pyridines.¹¹ Due to the hydrogen bonding, the carbohydrates stay specifically only in the pyridine domains surrounding PS domains within the coating. AAO pore channels confined the hydrogen-bonding self-assembly of PS-P4VP/carbohydrate within coatings, forming circular shapes similar to the preparation of one-dimensional mesoporous materials.¹² Due to the different self-assembly behavior of block copolymers, different pore structures and tube surface architectures (Figure 2a,d) have been obtained. Although the N position in the pyridine ring may affect the hydrogen bonding, the PS block sizes probably played a more important role in the control of pore structure and surface architecture. More work is underway to understand the formation of hollow structures by PS-P2VP on the tube wall. Annealing in solvent vapor was commonly used to promote the block copolymer microphase separation and refine the polymer nanostructure.¹¹ In this work, annealing of PS-P4VP/carbohydrate-coated AAO led to the formation of bamboo-like tube structure

with highly ordered, hexagonal nanopore arrays. High-temperature and long-time annealing in organic vapor probably promoted capillary forces within AAO pore channels, causing polymer/carbohydrates film attraction or coalescence across the as-prepared tube, which resulted in the formation of the bamboo-like structure after carbonization. Note that nanoporous blocks were formed like valves between the chambers, suggesting their potential applications in separation, controlled release, and storage. Functionalization of carbon nanotubes is a challenge for their wide range of applications.^{1–3} FTIR spectra (Supporting Information) of nanotubes carbonized at 460 °C and vacuum-dried overnight show hydroxyl bands between 3200 and 3600 cm^{-1} , which are attributed to free and hydrogen-bonded OH groups.^{11c} This suggests that these nanotubes can be further chemically functionalized through varied siloxane chemistry.¹³

Acknowledgment. We thank Todd Alam and Tim Boyle for their assistance on ^{13}C NMR and EA analysis. This work was partially supported by the U.S. Department of Energy (DOE) Basic Energy Sciences Program and Sandia National Laboratory's Laboratory Directed R&D program. TEM studies were performed in the Department of Earth and Planetary Sciences at The University of New Mexico. We acknowledge the use of the SEM facility supported by the NSF EPSCOR and NNIN grants. Sandia is a multiprogram laboratory operated by Sandia Corporation, a Lockheed Martin Company, for the U.S. DOE's National Nuclear Security Administration under Contract DE-AC04-94AL85000.

Supporting Information Available: Experimental details of the synthesis procedure; FTIR, ^{13}C NMR, and N_2 isotherms; and the thermogravimetric results. This material is available free of charge via the Internet at <http://pubs.acs.org>.

References

- (1) Ajayan, P. M.; Zhou, O. Z. *Carbon Nanotubes* **2001**, 80, 391–425.
- (2) Dai, H. J. *Acc. Chem. Res.* **2002**, 35, 1035–1044.
- (3) Hirsch, A.; Vostrowsky, O. *Funct. Mol. Nanostruct.* **2005**, 245, 193–237.
- (4) Kuzmany, H.; Kukovecz, A.; Simon, F.; Holzweber, A.; Kramberger, C.; Pichler, T. *Synth. Met.* **2004**, 141, 113–122.
- (5) (a) Iyer, V. S.; Vollhardt, K. P. C.; Wilhelm, R. *Angew. Chem., Int. Ed.* **2003**, 42, 4379–4383. (b) Rahman, S.; Yang, H. *Nano Lett.* **2003**, 3, 439–442. (c) Rajesh, B.; Thampi, K. R.; Bonard, J. M.; Xanthopoulos, N.; Mathieu, H. J.; Viswanathan, B. *J. Phys. Chem. B* **2003**, 107, 2701–2708. (d) Zhi, L. J.; Gorelik, T.; Wu, J. S.; Kolb, U.; Mullen, K. *J. Am. Chem. Soc.* **2005**, 127, 12792–12793. (e) Zhi, L. J.; Wu, J. S.; Li, J. X.; Kolb, U.; Mullen, K. *Angew. Chem., Int. Ed.* **2005**, 44, 2120–2123.
- (6) Kim, M.; Sohn, K.; Kim, J.; Hyeon, T. *Chem. Commun.* **2003**, 5, 652–653.
- (7) Arsenault, A. C.; Rider, D. A.; Tetreault, N.; Chen, J. I. L.; Coombs, N.; Ozin, G. A.; Manners, I. *J. Am. Chem. Soc.* **2005**, 127, 9954–9955.
- (8) Huck, W. T. S. *Chem. Commun.* **2005**, 4143–4148.
- (9) Li, W. H.; Wickham, R. A.; Garbary, R. A. *Macromolecules* **2006**, 39, 806–811.
- (10) Xiang, H.; Shin, K.; Kim, T.; Moon, S. I.; McCarthy, T. J.; Russell, T. P. *Macromolecules* **2005**, 38, 1055–1056.
- (11) (a) Sidorenko, A.; Tokarev, I.; Minko, S.; Stamm, M. *J. Am. Chem. Soc.* **2003**, 125, 12211–12216. (b) Liang, C. D.; Hong, K. L.; Guiochon, G. A.; Mays, J. W.; Dai, S. *Angew. Chem., Int. Ed.* **2004**, 43, 5785–5789. (c) Kosonen, H.; Valkama, S.; Nykanen, A.; Toivanen, M.; Brinke, G.; Ruokolainen, J.; Ikkala, I. *Adv. Mater.* **2006**, 18, 201.
- (12) (a) Ku, A. Y.; Taylor, S. T.; Loureiro, S. M. *J. Am. Chem. Soc.* **2005**, 127, 6934–6935. (b) Liang, Z. J.; Susha, A. S. *Chem.–Eur. J.* **2004**, 10, 4910–4914. (c) Wu, Y. Y.; Cheng, G. S.; Katsov, K.; Sides, S. W.; Wang, J. F.; Tang, J.; Fredrickson, G. H.; Moskovits, M.; Stucky, G. D. *Nat. Mater.* **2004**, 3, 816–822. (d) Yamaguchi, A.; Uejo, F.; Yoda, T.; Uchida, T.; Tanamura, Y.; Yamashita, T.; Teramae, N. *Nat. Mater.* **2004**, 3, 337–341. (e) Yao, B.; Fleming, D.; Morris, M. A.; Lawrence, S. E. *Chem. Mater.* **2004**, 16, 4851.
- (13) Fan, H. Y.; Lu, Y. F.; Stump, A.; Reed, S. T.; Baer, T.; Schunk, R.; Perez Luna, V.; Lopez, G. P.; Brinker, C. J. *Nature* **2000**, 405, 56–60.

JA061380C